Chapter 5

A QUANTITATIVE HEALTH MONITORING APPROACH USING IMPEDANCE SENSORS

5.1 Introduction

Due to the high frequency range employed, the impedance-based technique is very sensitive to minor changes in the near field of piezoelectric sensors. The sensitivity of this technique to local changes is very useful in most cases. However, due to the difficulties in developing an analytical model at such high frequency ranges, this technique can not correlate a change in electrical impedance with a specific change in structural properties, hence it only provides limited information on the nature of damage. In addition, to assess the life expectation of a structure, damage should be quantified and appropriate model is necessary for quantitative evaluation. This research is motivated by the necessity to combine the impedance-based health monitoring with a model-based damage detection technique in order to establish a more rigorous and quantitative health monitoring methodology.

This chapter describes the analysis of the performance of an integrated structural health monitoring method by combining the impedance-based method with a model-based technique. To quantitatively assess the state of a structure, a new model-based damage identification technique, based on a wave propagation approach, has been developed. Direct frequency response function data, as opposed to modal data, are utilized to characterize the state of the structure. A numerical example and an experimental investigation of one-dimensional structures are presented to illustrate the performance of this technique.

5.2 Wave Propagation model

Doyle (1997) has derived a spectral formulation for a dynamic finite element, referred to as the spectral finite element or the dynamic stiffness matrix formulation, which is suitable for high frequency analysis. Based on this approach, extensive theoretical modeling efforts have been made to identify the sensing region in the impedance-based structural health monitoring technique (Esteban, 1996). In addition, the wave element-by-element sensitivity approach is proposed and compared to a finite element model to validate the improved performance in detecting small mass or stiffness changes (Pines, 1997).

The spectral finite element method uses a formulation similar to that of the conventional finite element method, but the displacement is not assumed to be a polynomial form and the method treats the distributed mass and rotation inertia exactly, allowing elements to span from discontinuity to discontinuity. This has the advantage of reducing the number of elements used when compared to the conventional method, hence is computationally efficient for events involving high frequency excitations.

In the spectral method, the longitudinal displacements for bar can be written as,

$$u(x,w) = Ae^{-ikx} + Be^{-ik(L-x)} \tag{5.1}$$

where A and B are constants determined from the boundary conditions, ω is the radial frequency, and k is the wavenumber (1/length). By incorporating displacements, $u(x,w)$, into a generalized bar equation, the force-nodal displacements relationship can be established as,

$$\vec{F} = [z]\ \widetilde{u} \tag{5.2}$$

where,

$$[z] = \frac{EA}{L} \cdot \frac{ikL}{1 - e^{-i2kL}} \begin{bmatrix} 1 + e^{-i2kL} & -2e^{-ikL} \\ -2e^{-ikL} & 1 + e^{-i2kL} \end{bmatrix} \tag{5.3}$$

[Z] is referred as the local dynamic stiffness matrix, $\tilde{u}$ is the nodal displacement, L is the length of the bar element. The wavenumber is given by,

$$k = \omega \sqrt{\frac{\rho A}{EA}} \tag{5.4}$$

where ρA is the mass per unit length and EA represents the longitudinal stiffness of the element.

The local stiffness matrix of each element is obtained and then assembled into the global stiffness matrix. The compatibility of the local stiffness matrix is satisfied at the assembly stage by constraining each element displacement to match the displacement at the nodes. Hence,

$$\vec{F} = [\mathbf{Z}]\ \tilde{u} \tag{5.5}$$

where $[\mathbf{Z}]$ is the global dynamic stiffness matrix, which is the reciprocal of the transfer function. This matrix is symmetric and banded as in the case of conventional finite elements, but is frequency dependent. After application of the boundary conditions, the global dynamic stiffness matrix is constructed and the nodal displacements are found by inverting the matrix $[\mathbf{Z}]$. This is done at every discrete frequency for a frequency range of interest, therefore the displacements of each nodes at any frequency can be determined.

The other strength provided by the spectral modeling is that it can easily accommodate a higher order structural theory, such as the Mindlin-Herrmann model for rods and the Timoshenko model for beams, without adding extra degrees of freedom. In addition, the

responses at any location between the nodes are also easily computed using shape functions and the nodal values.

5.3 Damage Identifications using Frequency Response Functions

In recent years, several investigations have been made to utilize the measured frequency response function data, as opposed to modal data, for detecting damage in the structures (Zimmerman et al., 1995; Choudhury and He, 1996; Schulz *et al*., 1996; 1998). This technique has certain advantages over the modal domain approach, in that i) Each FRF contains information on all of the modes provide, ii) no analytical effort is needed to perform curve fitting, ii) there is abundant data, allowing judicious selection of frequency range. On the other hand, no curve fitting means that the FRF would still contain the effects of measurement noise.

In the wave finite element models, Pines (1997) showed that the damage could be modeled as a change in the local wavenumber in an individual element. A change in wavenumber is analogous to changes in mass and stiffness in modal based methods. Hence, damaged spectral element can be reconstructed as,

$$[Z]_d = \frac{EA}{L} \cdot \frac{i\alpha kL}{1-e^{-i2\alpha kL}} \begin{bmatrix} 1+e^{-i2\alpha kL} & -2e^{-i\alpha kL} \\ -2e^{-i\alpha kL} & 1+e^{-i2\alpha kL} \end{bmatrix} \tag{5.6}$$

where α represents relative change of a damaged wavenumber to an undamaged one. The undamaged and damaged response can be related by the force and displacement expressions as,

$$\vec{F} = [Z(\omega)]_d \tilde{u}_d = [Z(\omega)]_u \tilde{u}_u \tag{5.7}$$

using subscript *u* and *d* for the undamaged and damaged response, respectively. In addition, the difference between the damaged and undamaged dynamic stiffness matrix is calculated:

$$[\Delta Z(\omega)] = [Z(\omega)]_d - [Z(\omega)]_u \tag{5.8}$$

Here, ΔZ represents the effects of damage on the dynamic stiffness matrix. Incorporating equation (5.8) into the right side of equation (5.7) leads to the following relations,

$$[Z(\omega)]_d \tilde{u}_d = [[Z(\omega)]_u + [\Delta Z(\omega)]] \tilde{u}_d = [Z(\omega)]_u \tilde{u}_u \tag{5.9a}$$

$$[Z(\omega)]_u (\tilde{u}_u - \tilde{u}_d) = [\Delta Z(\omega)] \tilde{u}_d \tag{5.9b}$$

$$[Z(\omega)]_u \Delta\tilde{u} = [\Delta Z(\omega)] \tilde{u}_d = \{d(\omega)\} \tag{5.9c}$$

$d(\omega)$ is referred as *damage location vector* (DLV) at frequency ω. The location of damage could be identified by corresponding nonzero rows in $d(\omega)$, since they reflect nonzero terms of ΔZ in a specific element. DLV could be easily obtained with a model of the structure and the measured response. Note that this technique does not need information on the exciting force. The overall DLV is obtained as the average value of $d(\omega)$ over the measured frequencies,

$$D = \sum_{i=1}^{n} \frac{d_i(\omega_i)}{n} \tag{5.10}$$

where n is the number of frequency points measured.

The extent of damage, which means the value of α, can be obtained from the left side of equation (5.9c) with the substitution of $\Delta Z(\omega)$ with the representations in (5.3) and (5.6). This procedure can be applied only to the suspect element from the locating scheme. In fact, no closed form solution for α exists. However, using a Newton's secant method, the value of α can be easily obtained with quick convergence. This procedure is performed at each discrete frequency over the entire frequency range of interest, and finally a weighted average value is adopted for α to reduce random error (in the case of the noise present).

The damage location scheme presented herein is based on the approach developed by Choudhury and He (1996), adapted to utilizing the spectral element method. By spectral modeling, this approach could be extended to the high frequency analysis and found to be more computationally efficient than conventional finite element analysis.

5.4 Simulation Results

An example is presented to validate the method presented in the previous section. Our structure is a free-free bar as shown in Fig 5.1, which undergoes a longitudinal vibration and is modeled with ten elements.

Both damaged and undamaged responses are generated by ten spectral finite elements. Damage, a 10% increase in wavenumber, was introduced in the fifth element. This change is equivalent to a decrease in Young's Modulus by 20 % in one element, which induces a reduction of stiffness.

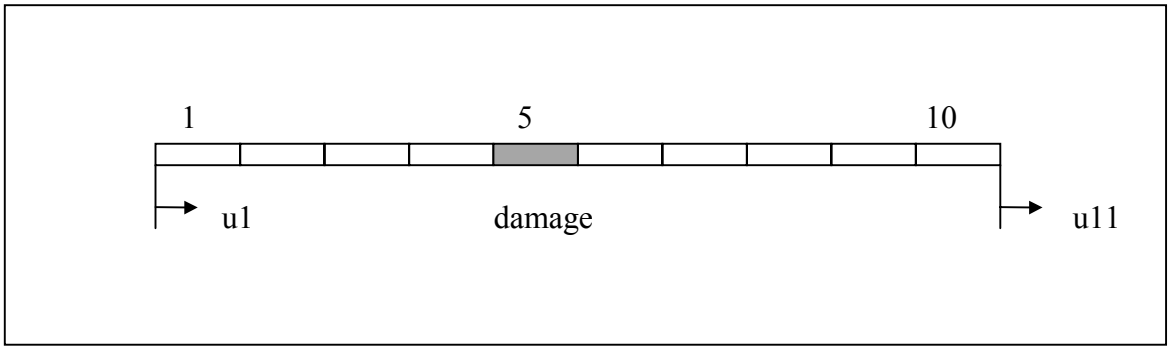

Figure 5.1 Free-Free bar with ten spectral elements

In noise-free cases, the exact location of the damage and a 10 % change in wavenumber of the fifth element were clearly identified. To simulate a more realistic situation, a random noise (5% noise to signal ratio) with Gaussian distribution is added to each of the damaged response curves. The damaged and undamaged responses of u_5 are shown in Fig 5.2. This plot shows from the fifth modes. There is a slight change in resonant frequencies, which suggests a change in stiffness of this structure.

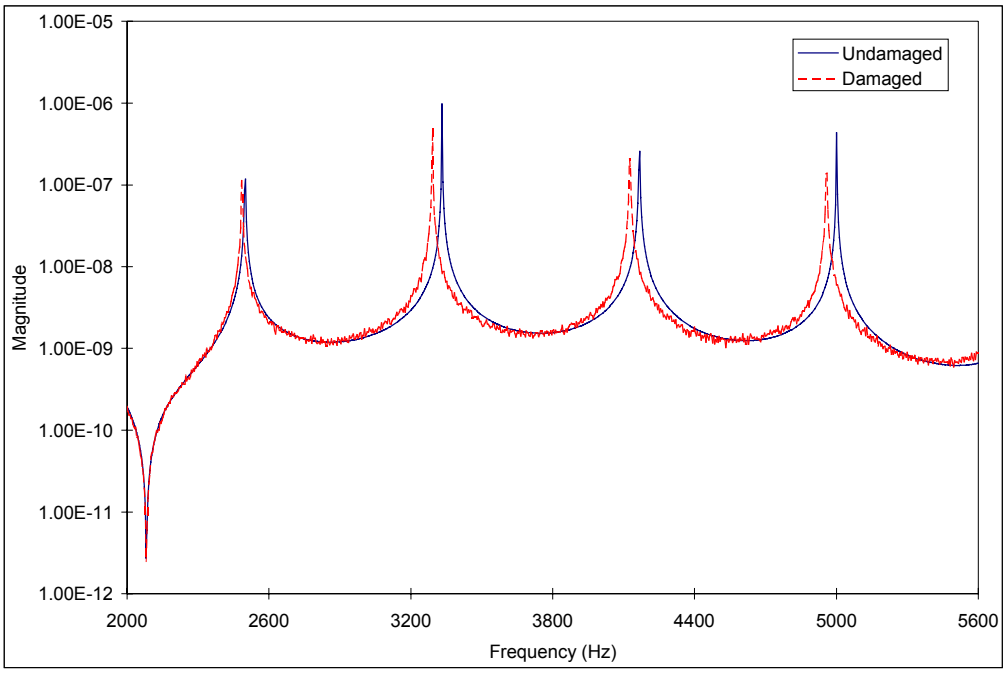

Figure 5.2 Response at u7 of free-free bar with noise added to the damaged response

As expected, the location of damage is clearly identified, as shown in Fig 5.3. A high value of DLV indicates damage at those degrees of freedom. The 5^{th} and 6^{th} dofs correspond to the element five. In addition, a 13 % change in wavenumber is identified, as shown in Figure 5.4. The estimated values are slightly higher with the noise present, but are in good agreement with the exact values.

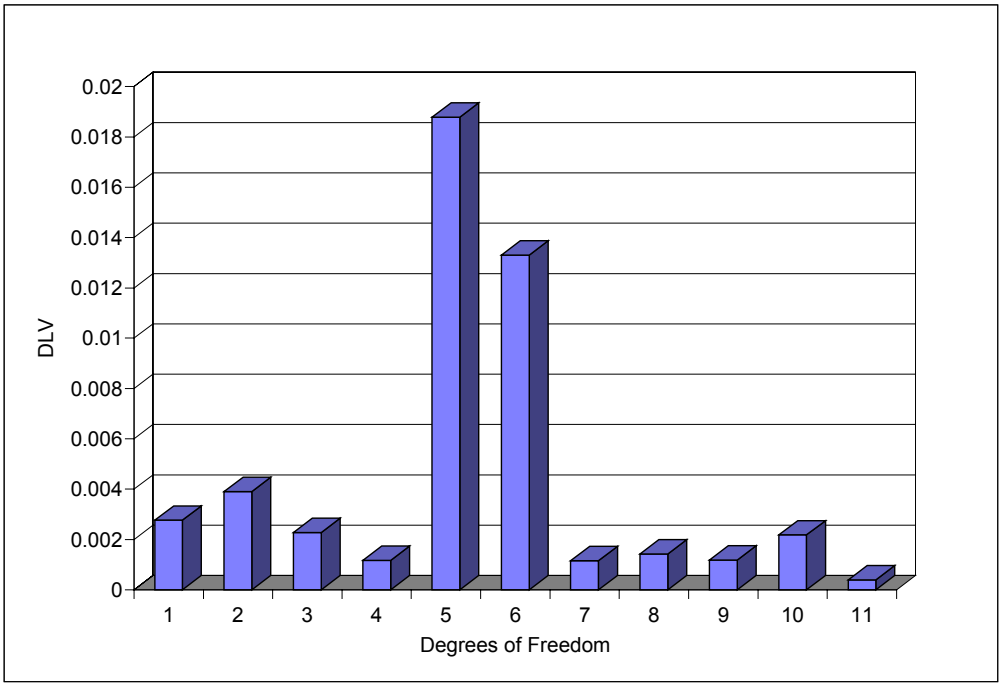

Figure 5.3 DLV Chart. The 5^{th} and 6^{th} dofs correspond to the element five.

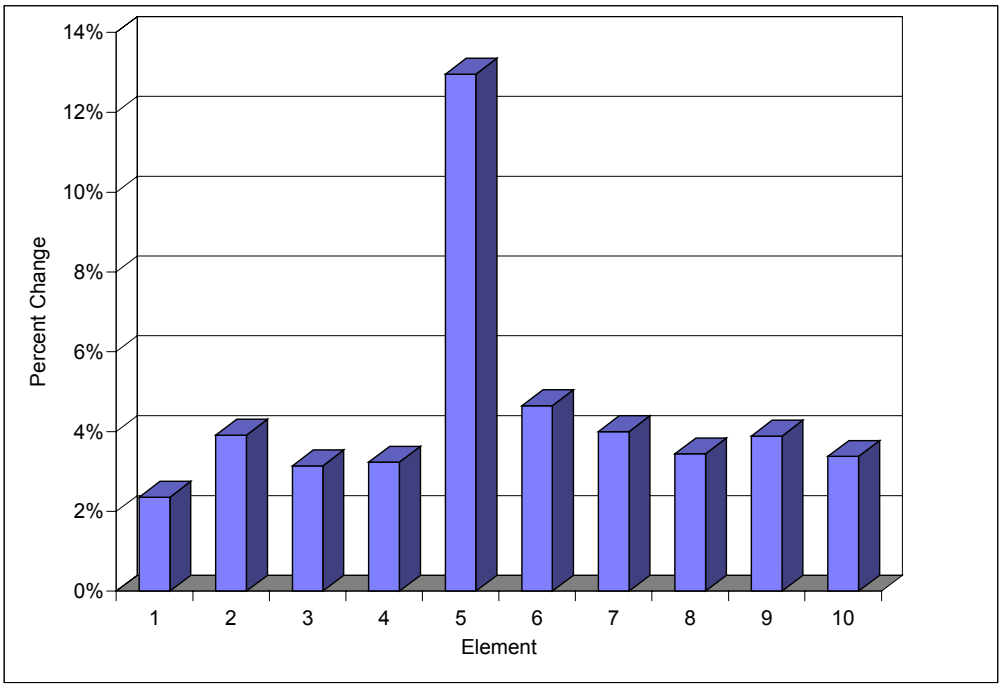

Figure 5.4 Percent Change in α . 13% change in Element 5.

5.5 Experimental Results

Experiments were performed to detect and locate damage in a free-free aluminum bar, as shown in Figure 5.5. Both the impedance-based method and the spectral-model based approach were applied to interrogate this structure. The aluminum bar is measured 630 x 40 x 2 mm and is suspended by a thin wire. Five PZT patches (30 x 30 x 1 mm) were boned to the bar, for the acquisition of electrical impedance and actuation of axial vibrations. An HP4194 electrical impedance analyzer was used for the measurement of the PZT's electrical impedance. A total of four spectral elements were constructed to model this structure and damage was induced by attaching two bolts on the third element. No assumption on the location or extent of damage was made, as is the case in practical health monitoring problems.

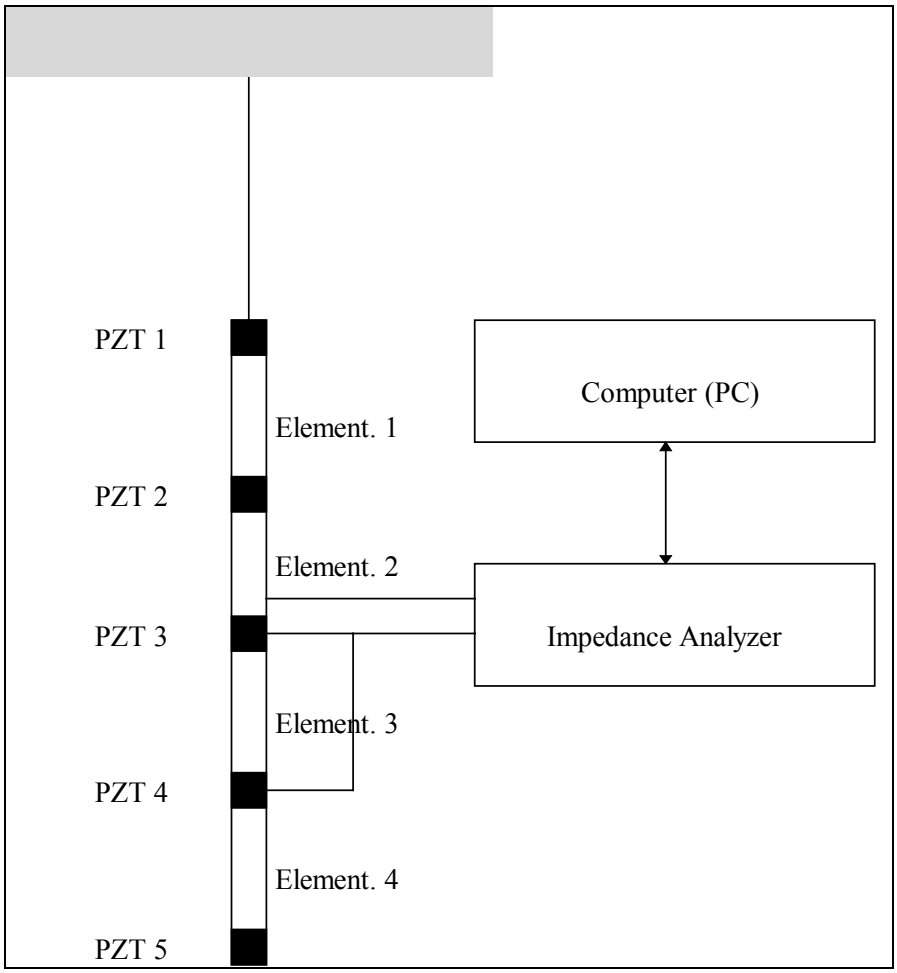

Figure 5.5 Experiement Setup

The impedance measurements of the PZT 3 over the 70 - 90 kHz frequency range are shown in Fig. 5.6. As can be seen, a complete change occurs in the signature pattern over the entire frequency range and is clearly indicative of damage. A damage metric chart is also shown in Fig 5.7. Damage metric, defined as the sum of the squared differences of the real impedance changes at each frequency step, is used to simplify the interpretation of the impedance variations and provides a summary of the information obtained from the each impedance response curve. As shown, there is a relatively large increase in the damage metric value for PZT's 3 and 4, which indicates damage is located between these two sensors. The other damage metric of three PZTs are also increased, and it could be stated that, despite the imited

sensing region of a PZT sensor in the impedance-based technique, only one PZT can be used to qualitatively monitor this specific structure.

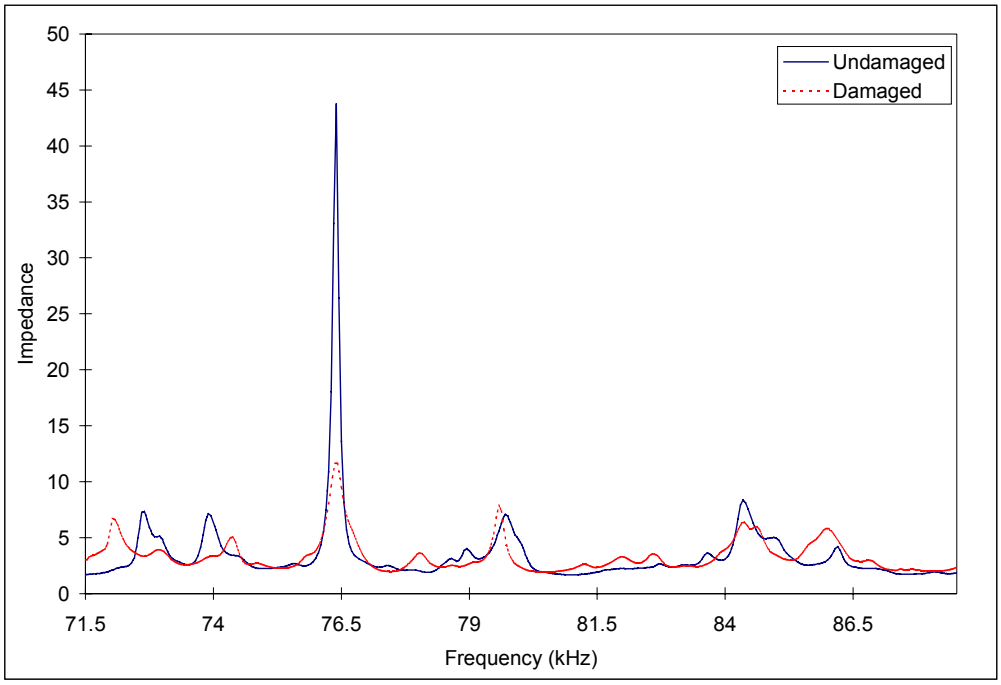

Figure 5.6 Impedance measurement of PZT 3 for both damaged and undamaged cases

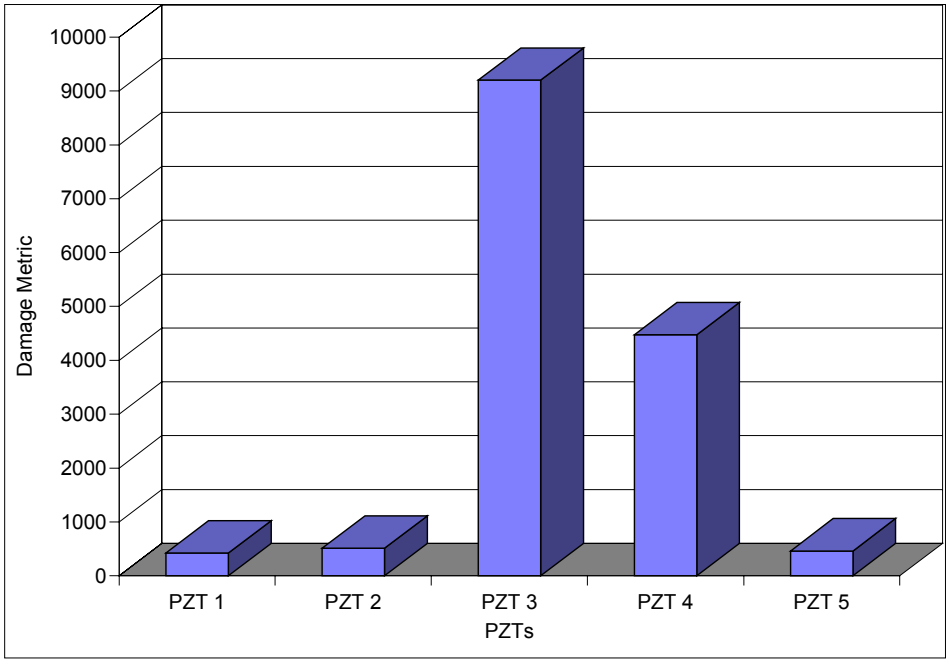

Figure 5.7 Damage Metric charts. PZT3 and PZT4 shows significant change, which in turn indicates damage is between these two sensors.

Simultaneously, the axial response of the bar is also measured using an attached accelerometer and the HP4194 analyzer. PZT patches are bonded on both sides of the bar, to ensure the actuation of longitudinal vibration. The response of u_2 and u_4 over the frequency range in 10 - 40 kHz are shown in Figure 5.8 and 5.9 for both the damaged and the undamaged case. As can be seen, although they are in good agreements, there is a slight discrepancy between the experimental and the analytical response. It is believed that the PZT's stiffening effect to the structure, which was not modeled in this study, causes this discrepancy. In addition, the signal from the accelerometer is very poor because the output of impedance analyzer is limited to 1 V maximum. The effects of modeling error and measurement noise, generally cause the modal analysis based techniques to have difficulties

in detecting structural damage, since they have to pick up very small changes in frequency or time responses. However in this proposed methodology, a damage location could be easily identified from the impedance-based technique, an analysis was carried out on the suspect element to estimate the extent of damage and 15% change in wavenumber on the third element was obtained. Considering the frequency ranges used in this experiment (10 - 40 kHz) and considering that only four finite elements where used to model this structure, the analytical predictions of damaged responses reasonably characterize the actual response of damaged structure, as shown in the figures.

This experiment provides an example of the applications of this integrated health monitoring system. With the impedance-based health monitoring technique, the PZT sensors/actuators would be installed in the critical section to monitor the condition of a structure. After acquiring the signals from each sensor, it would be possible in real-time to qualitatively detect and locate structural damage, where more detailed inspection would be carried out to estimate the severity of damage using this proposed technique.

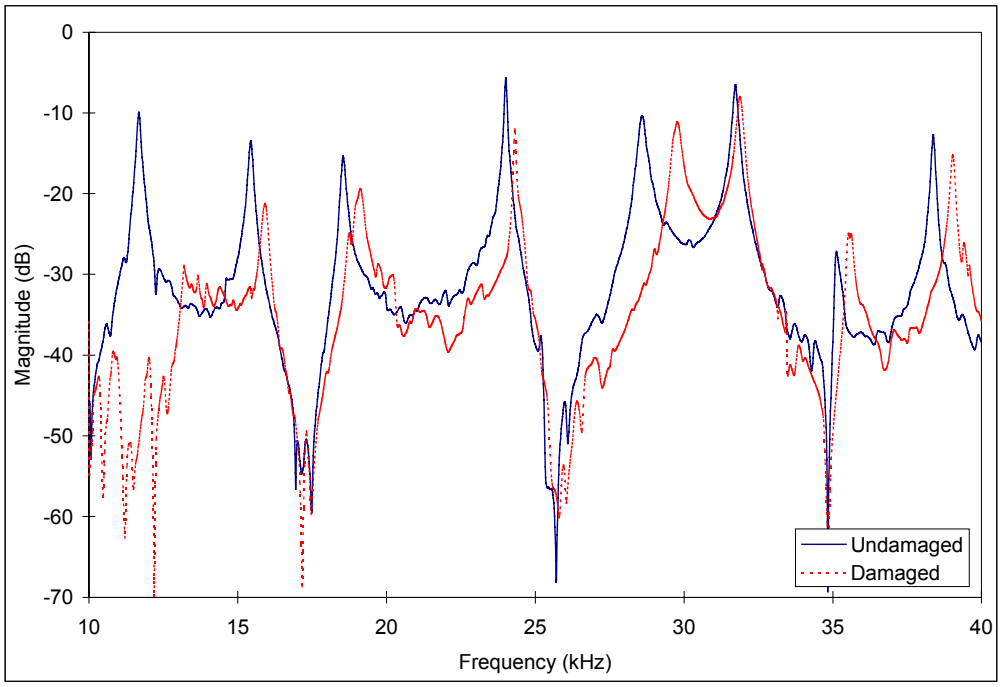

(a) Experimental results

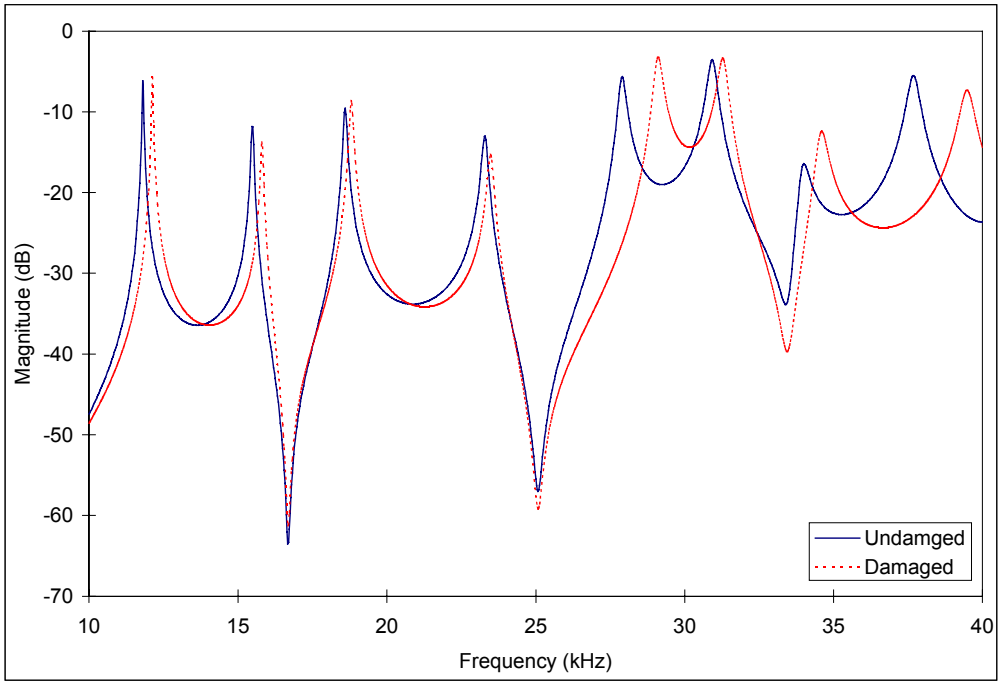

(b) Analytical results

Figure 5.8 The response of u2 from both simulation and experiment. 15% change in wavenumber (dashed) and undamaged curves (solid)

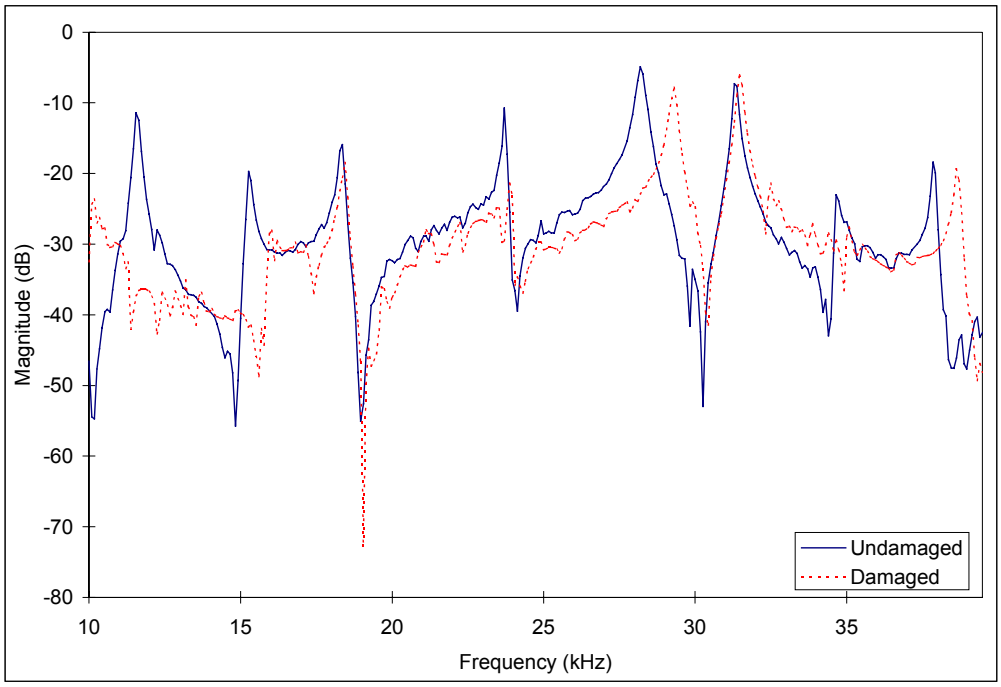

(a) Experimental results

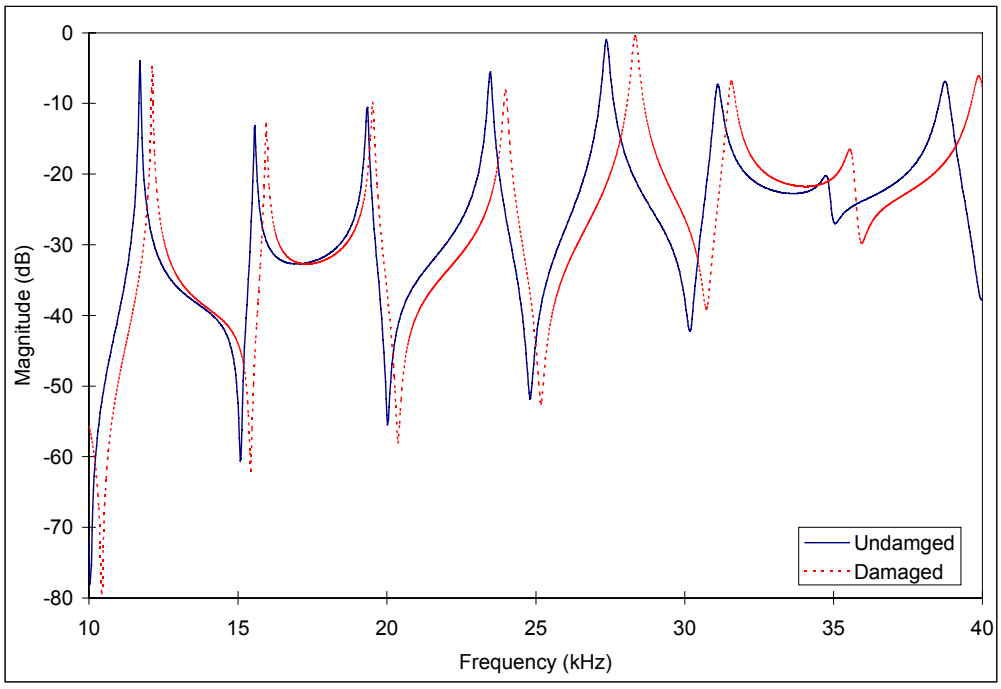

(b) Analytical results

Figure 5.9 The response of u4 from both simulation and experiment. 15% change in wavenumber (dashed) and undamaged curves (solid)

5.6 Summary

Contrary to most modal based NDE techniques, which rely on the lower order global modes, a combined approach utilizing high frequency excitation was presented. This technique would be more useful in identifying and tracking small defects, in the sense that damage is local phenomena and a high frequency effect.

In this methodology, two different damage detection schemes are integrated, including the impedance-based health monitoring technique and a wave propagation based approach. A new model based technique to detect structural damage at high frequency range was established for the quantitative assessment of structures. Measured frequency response function data were utilized to characterize the structural damage. By combining the advantages of the impedance method, this methodology will be able to provide an on-line structural health monitoring service and only perform the engineering analysis when known to be necessary.